Molecular Cell, Vol. 4, 935–947, December, 1999, Copyright ©1999 by Cell Press

The RAG1/RAG2 Complex Constitutes a 3′ Flap Endonuclease: Implications for Junctional Diversity in V(D)J and Transpositional Recombination

Sandro Santagata,* Eva Besmer,†‡ Anna Villa,§ Fabio Bozzi,§ John S. Allingham,‖ Cristina Sobacchi,§ David B. Haniford,‖ Paolo Vezzoni,§ Michel C. Nussenzweig,†‡ Zhen-Qiang Pan,* and Patricia Cortes†#

*Ruttenberg Cancer Center
Mount Sinai School of Medicine
1425 Madison Avenue
New York, New York 10029
†Laboratory of Molecular Immunology
‡Howard Hughes Medical Institute
The Rockefeller University
New York, New York 10021
§Department of Human Genome and Multifactorial Disease
Istituto di Tecnologie Biomediche Avanzate
Consiglio Nazionale delle Ricerche
via Fratelli Cervi 93
20090 Segrate (Milano)
Italy
‖Department of Biochemistry
University of Western Ontario
London, Ontario N6A 5C1
Canada

Summary

During V(D)J recombination, processing of branched coding end intermediates is essential for generating junctional diversity. Here, we report that the RAG1/RAG2 recombinase is a 3′ flap endonuclease. Substrates of this nuclease activity include various coding end intermediates, suggesting a direct role for RAG1/RAG2 in generating junctional diversity during V(D)J recombination. Evidence is also provided indicating that site-specific RSS nicking involves RAG1/RAG2-mediated processing of a localized flap-like structure, implying 3′ flap nicking in multiple DNA processing reactions. We have also demonstrated that the bacterial transposase Tn10 contains a 3′ flap endonuclease activity, suggesting a mechanistic parallel between RAG1/RAG2 and other transposases. Based on these data, we propose that numerous transposases may facilitate genomic evolution by removing single-stranded extensions during the processing of excision site junctions.

Introduction

The extensive repertoire of the antigen receptor is generated by both combinatorial and junctional diversity in a process known as V(D)J recombination. The rearrangement of variable (V), diversity (D), and joining (J) coding gene segments via site-specific recombination assembles the antigen-binding domains of immunoglobulin and T cell receptor molecules (Tonegawa, 1983). Processing of coding end intermediates introduces junctional diversity at the borders of the V, D, and J elements (reviewed by Lewis, 1994).

V(D)J recombination is guided by highly conserved recombination signal sequences (RSSs) comprised of a heptamer and a nonamer motif with an intervening 12– or 23–base pair spacer. Efficient rearrangement occurs only between RSSs with different spacer lengths; this phenomenon is known as the 12/23 rule (Tonegawa, 1983; Lewis, 1994; Eastman et al., 1996; Steen et al., 1996). Central to the rearrangement process are the two lymphoid-specific recombination activating genes, *RAG1* and *RAG2* (Schatz et al., 1989; Oettinger et al., 1990). In humans, mutations in either gene lead to profound defects in lymphopoiesis, manifested in severe combined immunodeficiency (SCID) (Schwarz et al., 1996) and Omenn syndrome (OS) (Villa et al., 1998). In mice, disruption of either RAG1 (Mombaerts et al., 1992) or RAG2 (Shinkai et al., 1992) leads to a complete block in both T and B cell development.

During the initial stages of the recombination reaction, RAG1/RAG2 form a complex with the RSS (Hiom and Gellert, 1997; Swanson and Desiderio, 1998; Santagata et al., 1998) that is in part stabilized by the interactions between the Hin-homologous region of RAG1 and the nonamer motif (Difilippantonio et al., 1996; Spanopoulou et al., 1996; Nagawa et al., 1998; Swanson and Desiderio, 1998) and between undefined domains of both RAG proteins and the heptamer motif (Eastman et al., 1999; Swanson and Desiderio, 1999). Bridging of 12 and 23 recombination signal sequences in a synaptic complex is critical for DNA cleavage and is facilitated by the DNA bending proteins of the HMG family (Sawchuk et al., 1997; Hiom and Gellert, 1998; Kim and Oettinger, 1998; West and Lieber, 1998; Aidinis et al., 1999).

Within the synaptic complex, RAG1/RAG2 efficiently introduce a nick at each RSS via a hydrolysis reaction at the heptamer/coding flank border, generating a 3′ hydroxyl end. Subsequently, a transesterification reaction creates a double-stranded (ds) break as the free 3′ hydroxyl of the nicked strand is used in a nucleophilic attack on the opposing strand, generating a covalently sealed hairpin intermediate (McBlane et al., 1995). The RAG and HMG proteins remain bound in a complex with the resulting 5′ phosphorylated blunt signal ends (Agrawal and Schatz, 1997) and the hairpin coding ends (Hiom and Gellert, 1998). The observed aberrant transposition of the blunt signal ends into plasmid acceptors in vitro implicates a role for RAG1/RAG2 in the evolutionary development of V(D)J recombination loci as well as in the generation of chromosomal translocations (Agrawal et al., 1998; Hiom et al., 1998). However, in vivo, transposition has not been observed and the reaction proceeds with both symmetrical and asymmetrical resolution of the hairpin coding ends. The ability of RAG1/

#To whom correspondence should be addressed (e-mail: cortep01@doc.mssm.edu). Present address: Immunobiology Center, Mount Sinai School of Medicine, 1425 Madison Avenue, New York, New York 10029.

RAG2 to nick DNA hairpins in vitro strongly suggests that they mediate hairpin opening via a hydrolysis reaction at this stage (Besmer et al., 1998; Shockett and Schatz, 1999). Tn10 uses a similar overall mechanism of hydrolysis, transesterification, and hydrolysis reactions during transposon excision (Kennedy et al., 1998).

The generation of junctional diversity is initiated by the asymmetric opening of hairpin coding intermediates to form single-stranded DNA (ssDNA) overhangs. In vivo, 3′ overhangs have been detected in pro-B cells undergoing recombination (Ramsden and Gellert, 1995; Livak and Schatz, 1997; Schlissel, 1998) while blunt ends and 5′ overhangs are also postulated to occur. At this stage, the open coding ends are potential substrates for nontemplated N nucleotide addition by terminal deoxynucleotidyl transferase (Landau et al., 1987), polymerase extension leading to P nucleotides, nuclease attack generating small coding element deletions, and microhomology-directed nonhomologous end joining (NHEJ) via annealing of short complementary stretches of the overhangs (Gerstein and Lieber, 1993; Ezekiel et al., 1997; Leu et al., 1997; Nadel and Feeney, 1997; Ramsden et al., 1997). These coding end intermediates, arising at this late stage of V(D)J recombination, have common branched structures characterized by duplex/single-strand (ds/ss) junctions lacking consensus binding motifs.

The V(D)J recombination reaction is concluded with the joining of the processed coding ends by the ubiquitously expressed double-strand break repair proteins Ku70/80, DNA-PK_{cs}, XRCC4 and ligase IV (reviewed by Lieber, 1999). Although it is not known when the double-strand break repair factors are incorporated into the recombination complex, it is plausible that they coexist with the RAG proteins during the generation of junctional diversity.

In this report, we demonstrate that the RAG1/RAG2 recombinase complex contains a structure-specific, sequence-independent 3′ flap endonuclease activity capable of removing single-strand (ss) extensions from a number of branched DNA structures. The ability to nick ds/ss junctions suggests a role for RAG1/RAG2 in generating both junctional and combinatorial diversity during the initial and final stages of V(D)J recombination. In addition, we identify an analogous activity for the bacterial transposase Tn10, suggesting a conserved role for a 3′ flap nuclease in mediating excision site junctional diversity in both V(D)J and transpositional recombination.

Results

RAG1 and RAG2 Cleave 3′ Overhangs at Duplex/Single-Strand Junctions

We have previously observed that RAG1 and RAG2 can mediate DNA hairpin opening (Besmer et al., 1998), suggesting that other coding end intermediates might also be processed by RAG1/RAG2. To examine this possibility, we tested in Mn^{2+} the capacity of the RAG1/RAG2 active cores to nick duplex oligonucleotide substrates containing 3′ single-strand overhangs ranging in length from 4 to 25 nucleotides. The overhangs were labeled at the 3′ end with ^{32}P cordycepin, and reaction products were resolved on denaturing polyacrylamide gels. Endonucleolytic incision was observed with each substrate tested with nicking directed to the ds/ss junction, independent of the nucleotide composition of the border (Figure 1B, lanes 2–6). Size markers (not shown) indicated that nicks were introduced either directly at the ds/ss border or 1 to 2 nucleotides within the double-strand portion of the structure (Figure 1A, arrows). The overhangs were released without evident 3′–5′ exonuclease degradation. Incubation of RAG1/RAG2 with substrates labeled at the 5′ end resulted in a complementary ladder of undegraded nicked 5′ fragments (data not shown). Only minor background nicking was noted when the strands were fully complementary (Figure 1B, lane 1).

This novel junction-dependent nuclease activity required both RAG1 and RAG2 as demonstrated using substrates −4 and −25 (Figure 1C, lanes 2–5 and lanes 8–11). Maximal nicking activity was obtained with RAG1/RAG2 complexes purified from extracts of cotransfected cells (Figure 1C, lane 6 and 12). Nicking of 3′ overhangs was also observed in Mg^{2+} (see Figures 2B, 2C, and 3B) albeit with 10-fold lower efficiency than in Mn^{2+} (data not shown).

We compared the products of overhang nicking by RAG1/RAG2 with those generated by mung bean nuclease, which leaves 3′ hydroxyl and 5′ phosphorylated ends. Comigration of the nicked overhangs with the mung bean nuclease–generated ladder (Figure 1B, lanes 2–5 and 7) and with phosphorylated oligonucleotide markers (data not shown) indicated that, like RSS nicking (Roth et al., 1993; Schlissel et al., 1993; McBlane et al., 1995) and hairpin opening (Besmer et al., 1998), 3′ overhang hydrolysis produces 3′ hydroxyl and 5′ phosphorylated ends. In addition, the ability of RAG1/RAG2 to nick by alcoholysis both RSSs (van Gent et al., 1996) and hairpins (Besmer et al., 1998) was maintained during the nicking of overhangs (Figure 1D). Treatment of the reaction on the −9 substrate with 12% and 20% 1,2 ethanediol (Figure 1D, lanes 3 and 7) or 12% and 20% glycerol (Figure 1D, lanes 4 and 8) produced slower migrating alcohol adducts. These findings indicate that RAG1/RAG2 contain a junction-dependent, sequence-independent endonuclease activity that can nick 3′ overhangs through alcoholysis, leaving 5′ phosphorylated and 3′ hydroxyl ends.

The Junction-Dependent Nuclease Is Formed by a Complex of RAG2 with the RAG1 C Terminus, Independent of the RAG1 Nonamer-Binding Domain

We examined the 3′ overhang nicking activity of two full-length RAG2 proteins containing mutations derived from a patient affected by OS. Due to the low nuclease activity of full-length RAG2 compared to that of the RAG2 active core, the assays were performed in the presence of Mn^{2+}. Nicking of the −25 substrate was either abolished or reduced significantly by substitutions C41W and M285R, respectively (Figure 2A, upper panel, lanes 3 and 4). 12 RSS-dependent nicking by these RAG2 proteins revealed activity levels corresponding to those observed on the −25 substrate, with C41W eliminating and M285R reducing RSS nicking (lower panel, lanes 3 and 4).

A panel of RAG1 mutations from OS and SCID patients

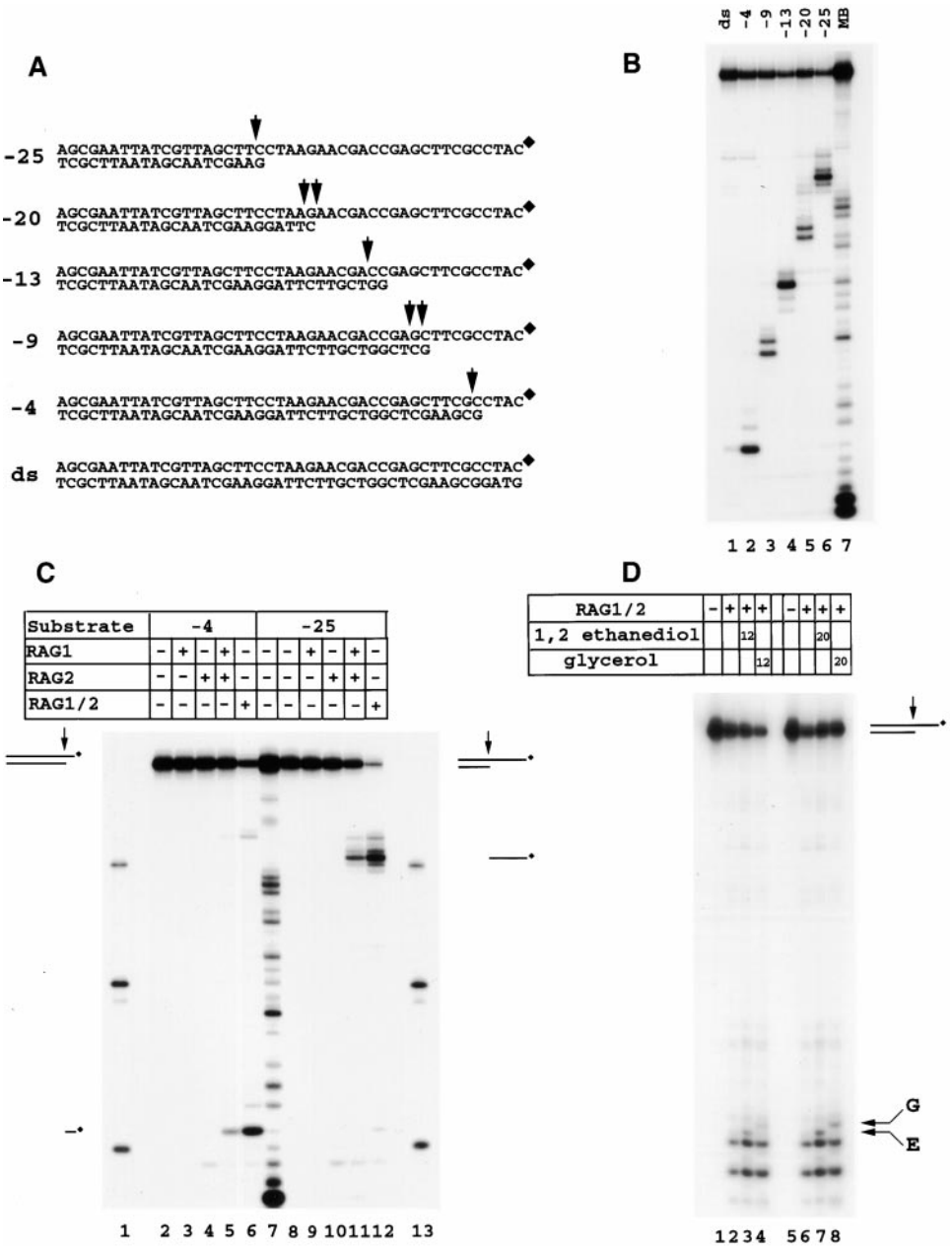

Figure 1. Endonucleolytic Nicking of 3′ Single-Stranded Overhangs by Core RAG1/RAG2

(A) Diagram of 3′ overhang substrates. The top strand was radioactively labeled at the 3′ end (diamond) with ^{32}P cordycepin. Arrows mark nicking sites.

(B) Junction-specific nicking by RAG1/RAG2. Nuclease assays were performed on substrates in (A) for 10 min at 37°C with coexpressed RAG1/RAG2 active cores in 2.5 mM Mn^{2+}. The DNA ladder (lane 7, MB) was generated by digesting substrate −25 with 10 units of mung bean nuclease for 1 min at 37°C.

(C) Nicking of 3′ overhangs is dependent upon both RAG1 and RAG2. Individual and copurified RAG proteins were assayed on substrates −4 and −25. Lanes 1 and 13 contain DNA size markers (5, 14 and 26 nucleotides) and lane 7 contains a mung bean nuclease generated ladder of substrate −25.

(D) Nicking at 3′ overhangs can be mediated by alcoholysis. The letters E and G identify ethanediol and glycerol adducts, respectively. Reactions contained 2.5 mM Mn^{2+}, coexpressed RAG1/RAG2 and ethanediol or glycerol at concentrations of either 12% or 20% on substrate −9.

was also analyzed for both structure-specific nicking of 3′ overhangs and sequence-specific nicking of the 12 RSS in the presence of Mg^{2+} (Figure 2B). Substitutions in the nonamer-binding domain (NBD) of RAG1 (R396H, S401P, R410Q, D429G and M433V) that have no effect on overhang nicking of the −25 substrate (Figure 2B, upper panels lanes 3–7) all decreased nicking of the 12 RSS to varying degrees (lower panel, lanes 3–7). This

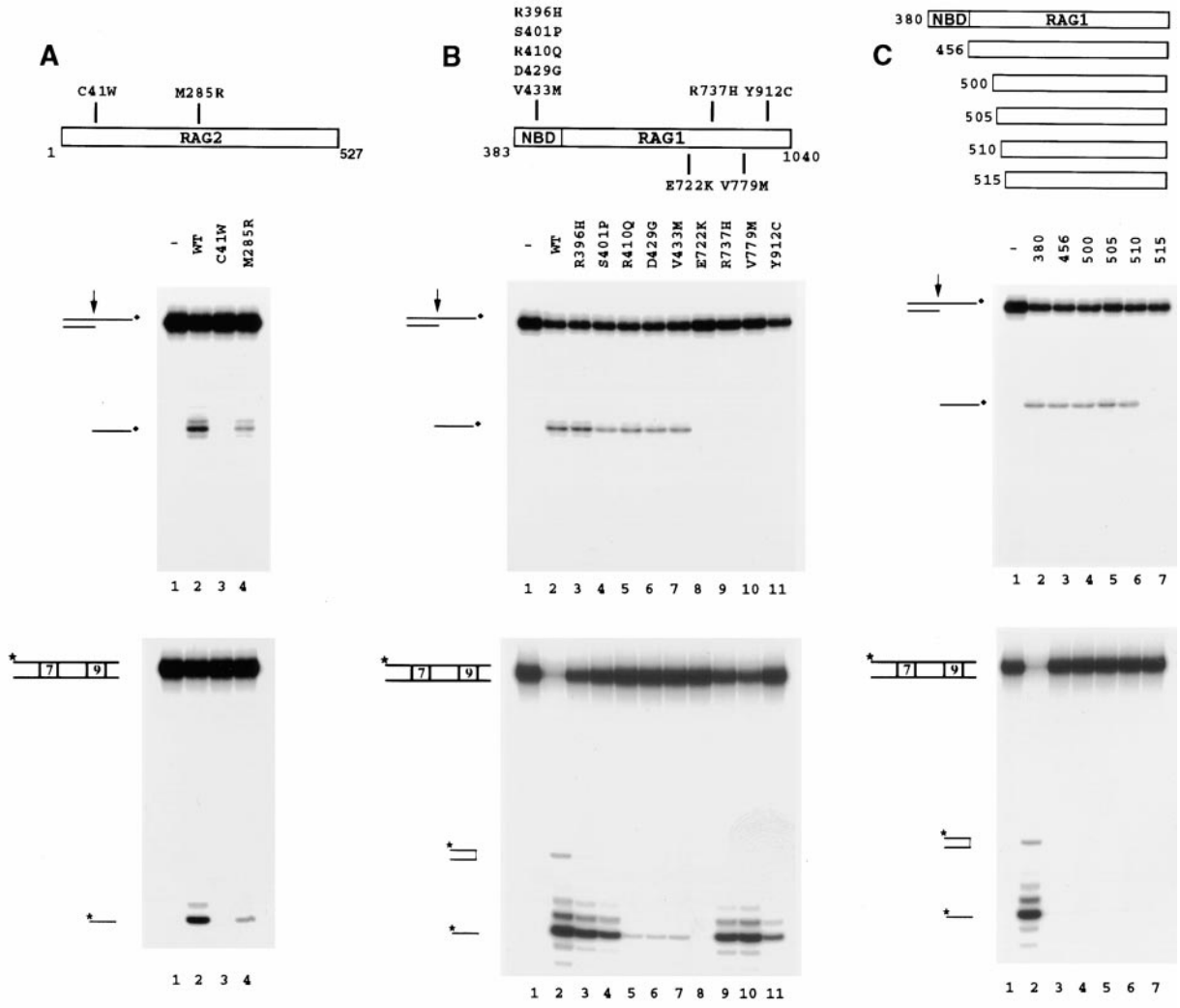

Figure 2. 3′ Overhang Nicking Activity Is Intrinsic to RAG1 and RAG2 but Independent of the RAG1 NBD

(A) Effect of point mutations within RAG2 (aa 1–527) on 3′ overhang and 12 RSS nicking. RAG2 substitutions C41W and M285R from patient OS1 (Villa et al., 1998) were coexpressed with wild-type core RAG1 (aa 380–1040) and incubated with substrate −25 in 2.5 mM Mn^{2+} (middle panel) or with 12 RSS in 1 mM Mg^{2+} (lower panel). Both substrates were incubated with RAG1/RAG2 for 20 min at 37°C.

(B) Differential effects of RAG1 amino acid substitutions on 3′ overhang and 12 RSS nicking. RAG1 alleles (aa 380–1040) from OS and SCID patients were coexpressed with wild-type core RAG2 (aa 1–383) and incubated with substrate −25 in 2.5 mM Mg^{2+} (middle panel) for 60 min or with 12 RSS in 2.5 mM Mg^{2+} (lower panel) for 10 min. NBD marks the RAG1 nonamer-binding domain.

(C) The RAG1 NBD is dispensable for structure-specific nicking of 3′ overhangs but is essential for sequence-specific 12 RSS nicking. Serial N-terminal deletions of wild-type core RAG1 (aa 380–515, upper panel) coexpressed with wild-type core RAG2 (aa 1–383) were assayed for nicking activity on both the −25 substrate for 60 min (middle panel) and on the 12 RSS for 10 min (lower panel). Both assays were conducted in 2.5 mM Mg^{2+} at 37°C.

suggests that the integrity of the sequence-specific recognition capacity of the NBD, although essential for RSS nicking, is not required for structure-specific nicking of 3′ overhangs. On the other hand, substitution E722K outside of the NBD eliminated 12 RSS nicking (lower panel, lane 8) and concomitantly abolished 3′ overhang nicking (upper panel, lane 8). Additional C terminal mutations—R737H, V779M, and Y912C—which reduced 12 RSS nicking by 60%–90%, abolished nicking of the −25 substrate. The apparent differential effect in these two activities is likely due to the efficiency of both reactions.

To confirm that the capacity for structure-specific nicking is localized to the C terminus of RAG1, progressive N terminal deletions were tested in Mg^{2+} for the ability to support nicking of the 12 RSS and the −25 overhang substrate. While the NBD (aa 396–456) was absolutely required for activity on the 12 RSS (Figure 2C, lower panel), nicking of the −25 substrate was NBD-independent (Figure 2C, upper panel), indicating that the N terminal 50% of RAG1 is nonessential for structure-specific nicking. In conclusion, junction-dependent endonucleolytic nicking activity is intrinsic to RAG1/RAG2 and is mediated by a complex between RAG2 and the C terminus of RAG1.

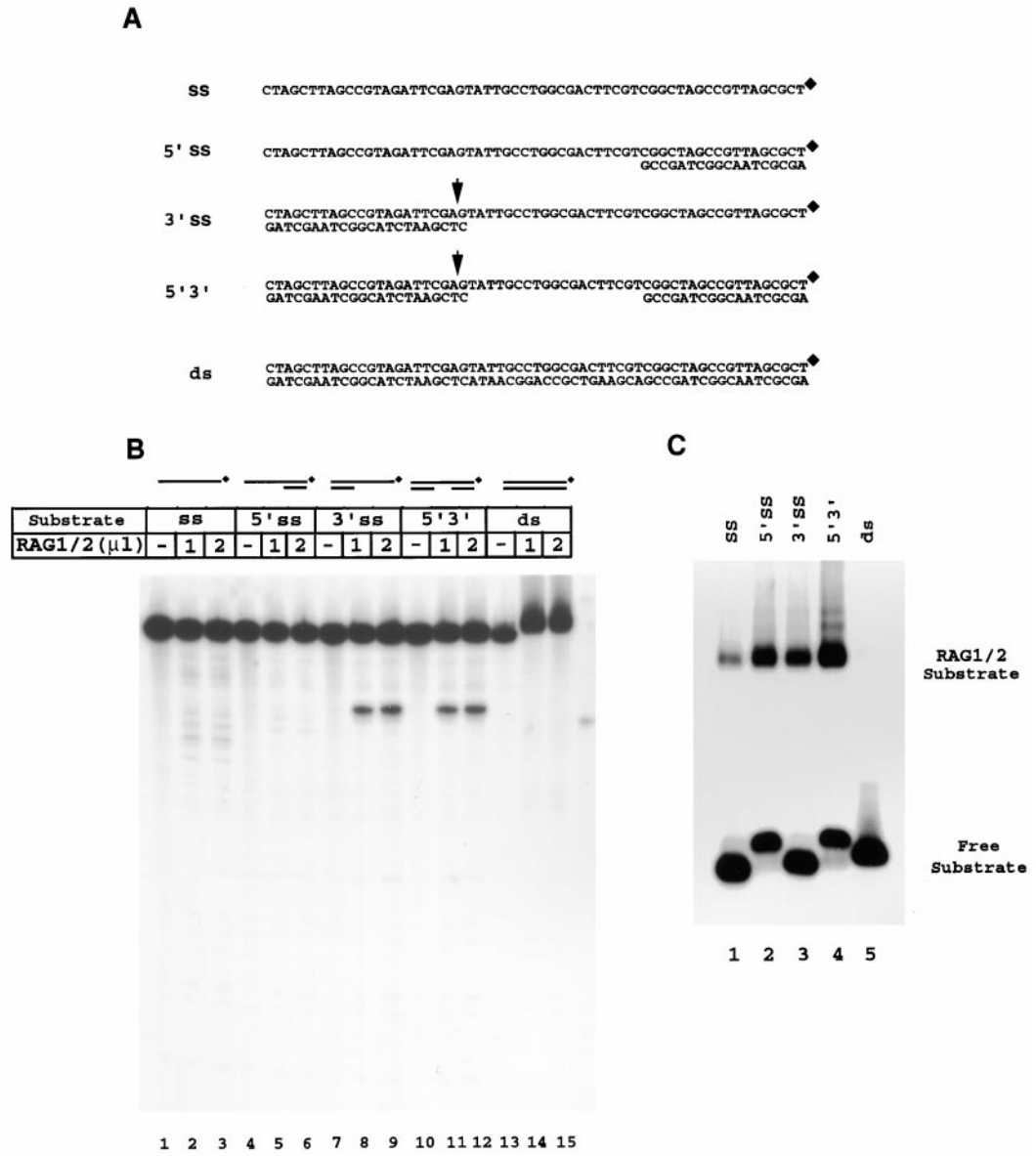

Figure 3. Binding of RAG1/RAG2 Is Stimulated by Both 5′ and 3′ ds/ss Junctions, but Nicking Is Activated Only by 3′ Overhangs

(A) Schematic of DNA substrates. The diamond marks the 3′ site of ^{32}P cordycepin addition. Arrows indicate the position of incision.

(B) Polar activation of RAG1/RAG2-mediated nicking by 3′ overhangs. Nuclease assays on substrates in (A) were conducted with coexpressed RAG1/RAG2 in 2.5 mM Mg^{2+} for 60 min at 37°C. The last lane contains a DNA marker (38 nucleotides).

(C) Mobility shift assay reveals polarity-independent stimulation of ds/ss transition recognition by RAG1/RAG2. Substrates were incubated with 100 ng of individually expressed RAG1 and RAG2 for 10 min at 30°C in 1 mM Ca^{2+} followed by cross-linking with 0.1% glutaraldehyde for 10 min at 30°C and resolution on a native 4% acrylamide gel.

Nicking at Overhang Junctions Demonstrates Distinct 3′ Polarity

To determine the polarity of ssDNA overhang processing by RAG1/RAG2, we employed a series of polar oligonucleotide substrates (Figure 3A). The substrates were either fully single-stranded, double-stranded, or had long 5′ (5′ss) or 3′ (3′ss) extensions. Substrate (5′3′) contained both 5′ and 3′ ds/ss junctions but had no accessible single-strand ends. Formation of the appropriate substrates was verified by either AluI or NheI digestion (data not shown). Nicking was observed only at the ds/ss junction with the 3′ overhang (Figure 3B, lanes 7, 8). Nicking at the 3′ overhang was not inhibited by blocking the free 3′ end with a complementary oligonucleotide (Figure 3B, lanes 11, 12), suggesting a free single-strand end is not required for accessing the 3′ ds/ss junction. We further investigated the ability of RAG1/RAG2 to recognize these substrates in mobility shift assays. The presence of a ds/ss junction of either polarity stimulated DNA recognition. Binding to substrates 5′ss and 3′ss

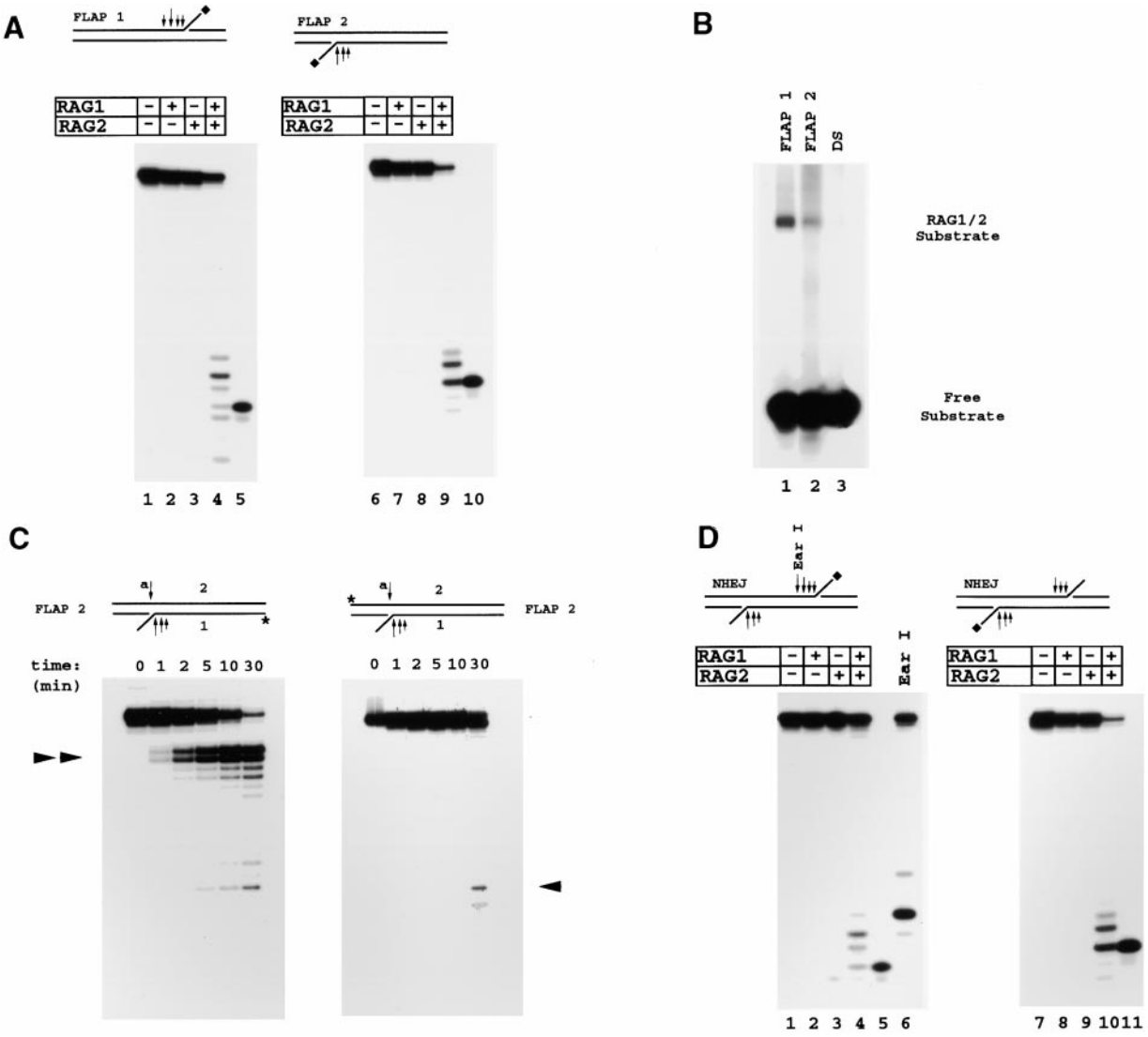

Figure 4. RAG1/RAG2 Constitute a 3′ Flap Endonuclease that Processes Branched DNA Intermediates

(A) Both RAG1 and RAG2 are required for structure-directed nicking of 3′ flaps. One hundred nanograms of RAG1 and RAG2 was incubated in 2.5 mM Mn^{2+} for 10 min at 37°C with substrate FLAP1 or FLAP2 3′ end labeled (diamond). Strong and weak incision sites are denoted by the length of the arrows on the substrate diagram. Lanes 5 and 10 contain 5- and 6-nucleotide size markers, respectively.

(B) Preferential recognition of flap DNA substrates by RAG1/RAG2. Mobility shift assays were conducted as outlined in Figure 3C.

(C) Kinetic analysis of nicking of FLAP2 reveals preference for flap arm removal over nicking across from the flap. Aliquots were collected over time from reactions with FLAP2 5′ end labeled (asterisk) either on strand 1 or 2. The double arrowhead indicates products formed after flap removal while incision across from the flap (at arrow a) is indicated by products marked by the single arrow. Reactions were performed in the presence of 2.5 mM Mn^{2+}.

(D) NHEJ substrates with 3′ branches are processed by RAG1/RAG2. Nucleotide size markers of 5 and 6 nucleotides are shown in lanes 5 and 11. Lane 6 of (E) contains substrate NHEJ digested for 1 hr with 5 units of EarI to confirm formation of the structure. Reactions were performed in the presence of 2.5 mM Mn^{2+}.

following glutaraldehyde cross-linking was 25-fold greater than binding to double-stranded DNA (dsDNA) and 5-fold increased over ssDNA (Figure 3C, lanes 1–3). Recognition of substrate 5′3′ was at least 2-fold greater than either 5′ss or 3′ss (Figure 3C, lane 4), suggesting that a free 3′ or 5′ end is not required for recognition of ds/ss junctions. We conclude that RAG1/RAG2 preferentially bind ds/ss junctions in a manner independent of polarity and the presence of a free 5′ or 3′ end. However, only 3′ overhangs activate RAG1/RAG2-mediated nicking.

The RAG1/RAG2 3′ Flap Endonuclease Processes NHEJ Structures In Vitro

We next determined the ability of RAG1/RAG2 to process complex-branched DNA structures. When incu-

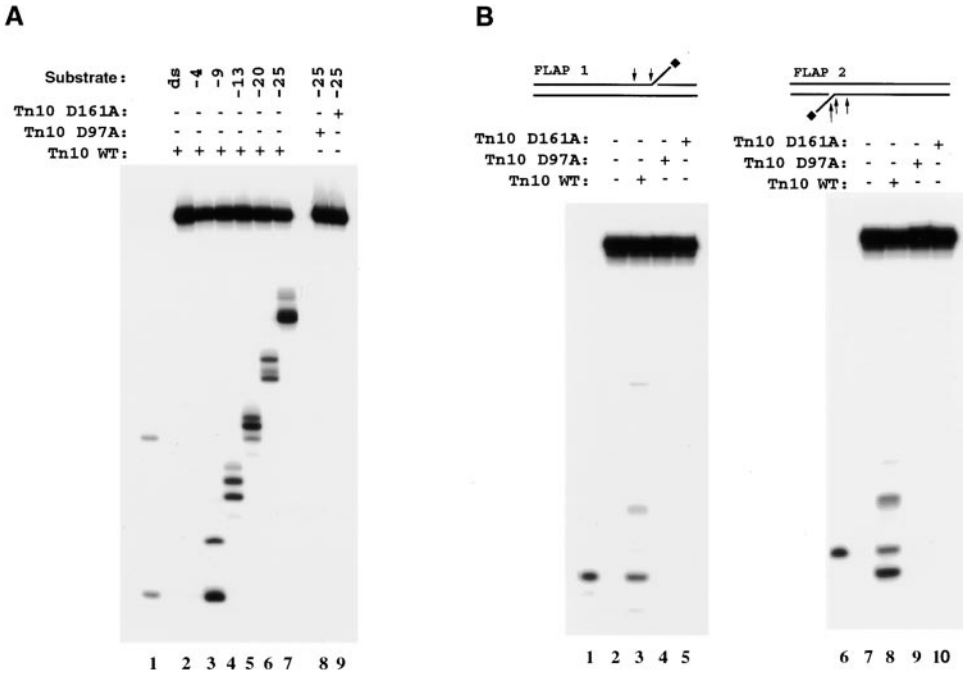

Figure 5. Bacterial Transposase Tn10 Is a 3′ Flap Endonuclease

Wild-type and mutant Tn10 proteins were incubated with (A) 3′ end labeled overhang substrates (from Figure 1A) and (B) substrates FLAP1 and FLAP2 (from Figure 4A) for 2 hr at 37°C in 5 mM Mn^{2+}.

bated with two different flap structures (FLAP1 and FLAP2) in 2.5 mM Mn^{2+}, RAG1/RAG2 effectively nicked the 3′ extensions (Figure 4A, lanes 4 and 9). This activity was heterogeneous in both efficiency (lanes 4 and 9) and site selection, which ranged from the precise junction of the flap to 3 nucleotides within the dsDNA. Minor nicking in the single-strand region was also observed. Gel shift analysis revealed that the binding to FLAP1 and -2 was enhanced 7 to 10-fold over double-stranded DNA with the same sequence (Figure 4B, DS DNA lane 3). Consistent with the absence of RAG1/RAG2 processing of 5′ overhangs (Figure 3B), we could not detect 5′ flap nicking (data not shown).

One complication of these 3′ flap substrates is that the continuous strand might be nicked across from the flap arm (Figure 4C, arrow a) to create a double-strand break and generate a 3′ overhang substrate. In turn, the observed nicking in Figure 4A might represent 3′ overhang rather than 3′ flap nicking. To address this possibility, we analyzed the kinetics of strand nicking of substrate FLAP2, 5′ end labeled on either the flap strand (1) or the continuous strand (2). After 30 min, over 95% of the flap strand (1) was nicked while less than 3% of the continuous strand (2) was nicked. Thus, nicking by the RAG1/RAG2 structure-specific 3′ flap endonuclease is predominantly directed to the 3′ flap.

The formation of coding joints both in vivo (Gerstein and Lieber, 1993; Gauss and Lieber, 1996; Ezekiel et al., 1997; Schlissel, 1998) and in vitro (Leu et al., 1997; Ramsden et al., 1997) is often guided by microhomologies between the two coding ends, presumably by the annealing of regions of short homology and subsequent removal of resulting flaps in a process paralleling NHEJ in yeast (Milne et al., 1996). We recreated complex-branched structures representing postulated end joining intermediates. While in vivo microhomologies typically range from 2 to 3 nucleotides, the limitations of oligonucleotide annealing in vitro required the use of an 11–base pair complementary region. Formation of the expected structure was verified by cleavage within the annealed central portion with EarI (Figure 4D, lane 6). RAG1/RAG2 removed both flaps (Figure 4D, lanes 4 and 10) with the same site variability as demonstrated for substrates FLAP1 and -2 (Figure 4A). The data suggest that RAG1/RAG2 form a 3′ flap endonuclease that can effectively process the proposed intermediates of microhomology-directed end joining.

The 3′ Flap Endonuclease Activity Is Conserved in the Bacterial Transposase Tn10

Similarities have been described between the DNA recognition, cleavage, and transposition activities of RAG1/RAG2 and those of DNA transposases, recombinases, and integrases. To address whether the 3′ flap nuclease activity is also maintained between RAG1/RAG2 and transposases, we assayed the bacterial transposase Tn10 for the capacity to nick the 3′ overhang substrates diagrammed in Figure 1A. Strikingly, Tn10 nicked 3′ overhang structures specifically at the junctions of dsDNA and ssDNA (Figure 5A), essentially reproducing the pattern generated by RAG1/RAG2. Nicking by Tn10 demonstrated 3′ polarity (data not shown). In addition, Tn10 removed 3′ flaps from both the FLAP1 and -2 structures. These activities are intrinsic to Tn10, as

aspartate-to-alanine substitutions of either active site residue D97 or D161 (Bolland and Kleckner, 1996) entirely abolished 3′ nicking (Figure 5A, lanes 8 and 9 and Figure 5B, lanes 4, 5, 9, and 10). We conclude that the ability to remove 3′ overhangs and flaps is conserved from bacterial transposases through mammalian recombinases.

Distortion of the Coding Flank/Heptamer Border Activates the 3′ Flap Nuclease Activity of RAG1/RAG2

We explored the role of the RAG1/RAG2 3′ flap endonuclease activity in heptamer nicking during the initial stages of V(D)J recombination. Since CACA sequences form an unusual DNA structure with a propensity for local unwinding (Patel et al., 1987), it has been suggested that RAG1/RAG2 binding to the RSS amplifies inherent local distortion within the heptamer and generates a single-stranded intermediate to ultimately facilitate DNA nicking (Cuomo et al., 1996; Ramsden et al., 1996). Indeed, copper phenanthroline footprinting (Akamatsu and Oettinger, 1998) and potassium permanganate modification experiments (Swanson and Desiderio, 1998) have provided direct evidence that RAG1/RAG2 alter the local structure at the heptamer/coding flank border. Such localized distortion may in effect create a flap-like ds/ss junction that might be sufficient for triggering nicking.

To study the effect of DNA distortion at the coding flank/heptamer border, we dramatically reduced RSS nicking by mutating the first two nucleotides of the heptamer (Figure 6A, MUT) in a fully double-stranded RSS (Figure 6B, lanes 1 and 2). In the context of this mutant heptamer, nucleotide changes in the lower strand were introduced to generate areas of localized DNA distortion (Figure 6A). Strikingly, in the presence of 2.5 mM Mg^{2+}, if 3 bases of the lower strand were changed to create a mismatch (MIS 1/3) at the coding flank/heptamer border, RSS nicking was activated 25-fold (Figure 6B, lane 3). Apparently, heptamer nicking can be triggered by the appropriate bubbled/flap-like structure. Under the same conditions, MIS 1/3 was nicked 2-fold more efficiently than substrate −25 and 4-fold more efficiently than FLAP1 (data not shown). Mismatch of only 1 nucleotide (MIS 1) was sufficient to boost nicking by RAG1/RAG2 (Figure 6C, lane 4). The position of the mismatch was found to be critical since a 3-nucleotide bubble in either the coding flank (MIS −3/−1) (Figure 6D, lane 3) or the spacer (MIS 7/9) (lane 6) did not resuscitate the mutated heptamer. However, a mismatch at positions 4–6 of the heptamer (MIS 4/6) triggered RAG1/RAG2-mediated nicking albeit inappropriately displaced by 1 nucleotide (lane 5). Nicking was invariably directed to the upper strand (Figure 6D); nicking of the lower strand was not observed for any of the mismatched substrates (Figure 6D, lanes 7–11), suggesting that the 3′ flap activity is restricted when the RAGs are bound to the RSS.

Mobility shift analysis showed that binding to the double-stranded mutant RSS (MUT) was stimulated over 30-fold by the introduction of a mismatch at the coding flank/heptamer border (MIS 1/3) (Figure 6E, lanes 2 and 3). Formation of this complex was 6- to 8-fold more efficient than with a double-stranded wild-type 12 RSS (Figure 6E, lanes 1 and 3). These relative binding efficiencies were confirmed by competing binding on both the wild-type and MIS 1/3 RSSs with either unlabeled wild-type or MIS 1/3 RSSs (data not shown). In accordance with the nicking data, the efficiency of RAG1/RAG2/RSS complex formation increased as more bases were mismatched (Figure 6F). Additionally, activation of binding was dependent upon the position of the DNA distortion as mismatches in the coding flank (MIS −3/−1) or spacer (MIS 7/9) had only minimal stimulatory effects (Figure 6G). Consistent with recent findings demonstrating that RAG2 is required for the promotion of heptamer occupancy (Eastman et al., 1999; Swanson and Desiderio, 1999), binding of RAG1 alone to the RSS was not stimulated by any of the mismatched substrates (data not shown). The data thus suggest that DNA distortion generating a flap-like ds/ss junction at the coding flank/heptamer border activates RSS recognition and nicking by RAG1/RAG2.

Discussion

The results presented in this report identify the RAG1/RAG2 recombinase as a 3′ flap endonuclease capable of removing single-strand extensions from the 3′ overhang, flap, and NHEJ structures that are central to the production of junctional diversity. The recombinase complex preferentially binds these branched structures independent of the RAG1 NBD and mediates nicking by hydrolysis or alcoholysis. Distortion of DNA at the coding flank/heptamer border activates RSS binding and nicking, suggesting a mechanism by which RAG1/RAG2 nick a flap-like ds/ss junction. These findings demonstrate that RAG1/RAG2 possess the requisite nuclease activity to generate both combinatorial and junctional diversity during the initial and final stages of the V(D)J recombination reaction. Moreover, the data suggest that the hydrolytic activity of the RAG1/RAG2 active site is triggered by recognition of a common ds/ss junction motif. Identification of a 3′ flap endonuclease activity in the bacterial transposase Tn10 highlights the conservation of junction-directed nicking activity among transposases and suggests that other transposases may utilize this activity during excision site processing.

Role of the RAG1/RAG2 3′ Flap Endonuclease in the Generation of Junctional Diversity

The resolution of coding end hairpins could yield two classes of asymmetrically nicked products (Figure 7A, structures A and B), the processing of which generates junctional diversity (Besmer et al., 1998; Shockett and Schatz, 1999; E. B. and P. C., unpublished data). A nick (blue arrow) generating a 5′ overhang and a recessed 3′ hydroxyl group (structure A) provides a substrate for polymerase extension leading to P nucleotide introduction. Consistent with this, RAG1/RAG2 do not remove 5′ overhangs (Figure 3B). Once extended, the newly formed blunt coding end can be ligated with another blunt coding end intermediate (PATH I) to form a bona fide coding junction. Alternatively, nicking (red arrow) on the opposing face of the hairpin produces a 3′ overhang with a recessed 5′ end (structure B). While this substrate cannot be extended by polymerases, it can

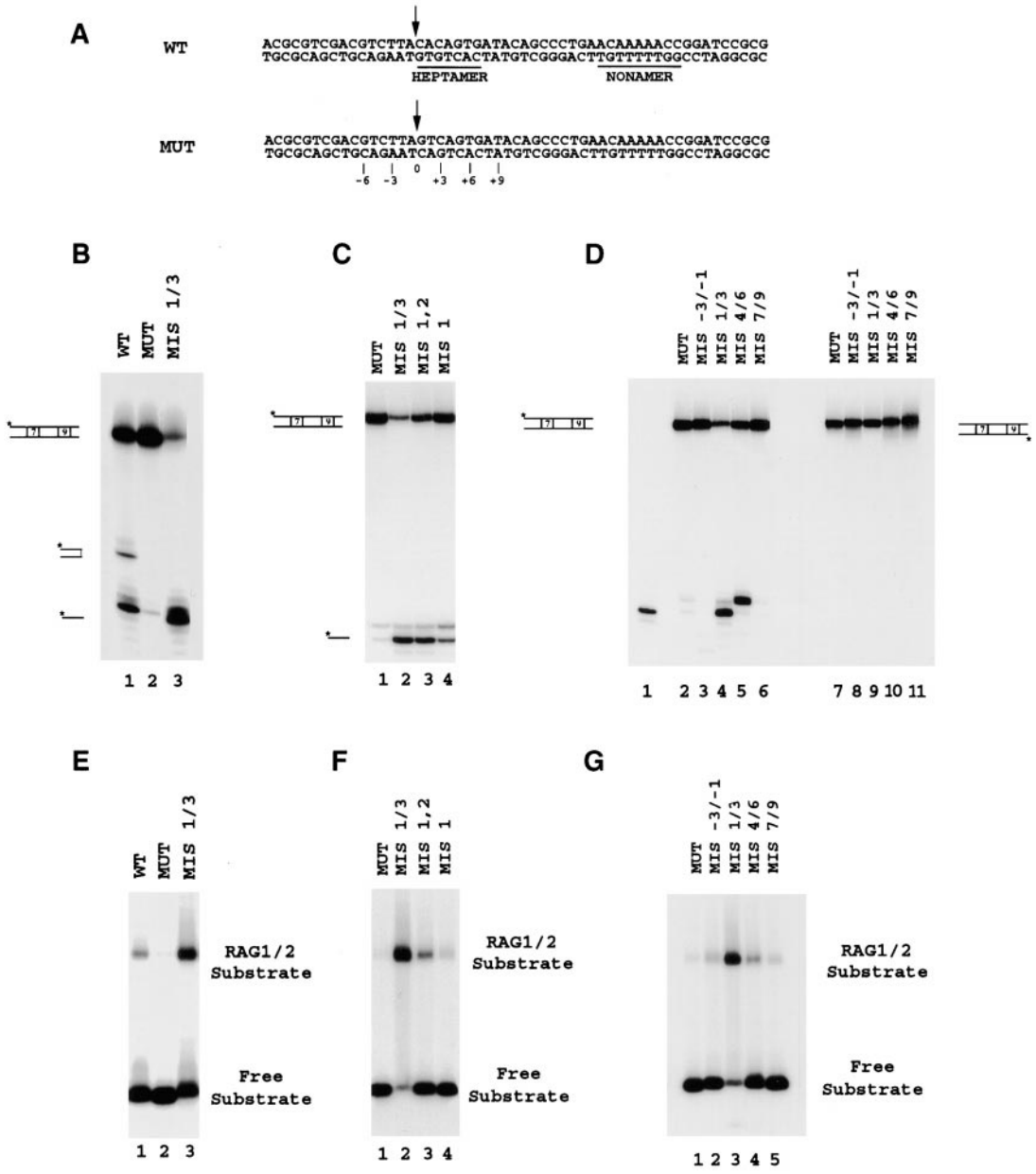

Figure 6. Mismatches at the 12 RSS Coding Flank/Heptamer Border Stimulate Recognition and Site-Specific Nicking by RAG1/RAG2

(A) Diagram of 12 RSS substrates. Arrows indicate site of DNA nicking. The sequence of wild-type and mutant (first CA of the heptamer to GT) 12 RSSs is displayed. Nucleotide positions are indicated with position 0 assigned to the site of nicking. In B–G, substrate MUT was generated by annealing the mutant 12 RSS with a fully complementary lower strand. Mismatched substrates were formed by annealing the mutated upper strand 12 RSS with lower strand oligonucleotides containing mismatches at the indicated positions.

(B) A 3-nucleotide bulge within the heptamer at the coding flank/heptamer border reactivates nicking of a mutated heptamer. Reactions were conducted in 2.5 mM Mg^{2+}.

(C) A mismatch of 1 nucleotide is sufficient to reactivate DNA nicking.

(D) Stimulation of nicking is limited to nucleotide mismatching within the heptamer motif and is directed strand specifically.

(E–G) Enhanced recognition of mismatched heptamers by RAG1/RAG2.

be processed by at least three different mechanisms (Figure 7A, PATHS II–IV) involving the RAG1/RAG2-mediated, junction-specific nuclease activity revealed in Figure 1B.

In the absence of prior ligation, short deletions can be introduced when a free 3′ overhang (structure B) is removed by RAG1/RAG2 (see Figures 1–3) yielding a suitable substrate for polymerase extension and end ligation (PATH II). In PATH III, following lower strand ligation with another blunt coding end (structure C), short deletions can be generated by removal of the short 3′ flap of the upper strand (see Figure 4A). Alternatively,

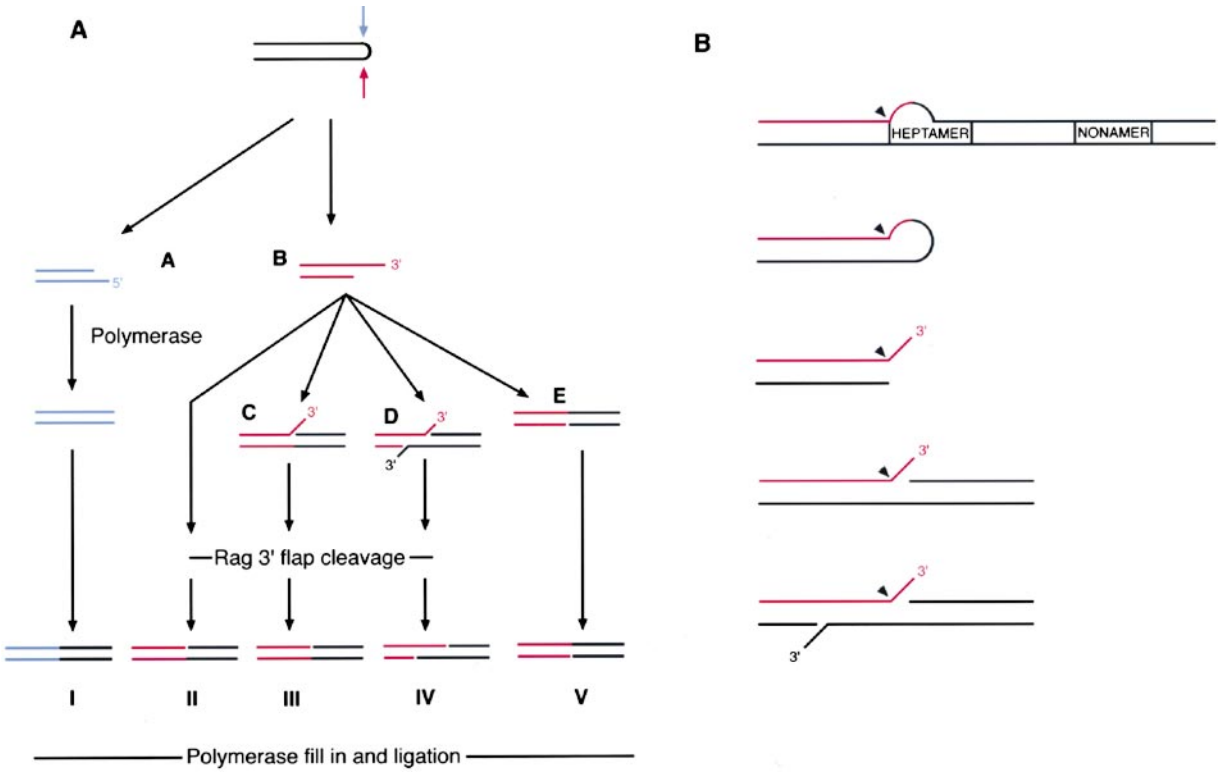

Figure 7. Implications of RAG1/RAG2-Mediated Nicking at ds/ss Junctions
(A) Model for the role of RAG1/RAG2 3′ flap endonuclease activity in alternative paths of coding end processing (see Discussion for details).
(B) Model for the activation of RAG1/RAG2-mediated nicking by the common structural determinants (indicated by darts) at ds/ss junctions.

if 3′ overhangs share regions of nucleotide homology, end migration could facilitate the formation of NHEJ structures (structure D; PATH IV). The 3′ nuclease activity of RAG1/RAG2 can resolve such structures by removing the 3′ extensions (Figure 4D), ultimately permitting ligation and completion of the recombination process. The resulting coding joint would contain both P nucleotides and short deletions. Another path proceeding in the absence of RAG1/RAG2 flap nicking could involve single-stranded ligation via the hydroxyl group of the 3′ overhang and the 5′ phosphate of another blunt coding end to yield a gap (structure E) to be filled in by a polymerase (PATH V; Schlissel, 1998). In this case, P nucleotides would be contributed in the absence of any deletions.

These mechanisms can account for the short deletions observed at the coding borders, for the resolution of NHEJ intermediates directed by short stretches of sequence homology, and for the addition of P nucleotides. While the presence of RAG1/RAG2 in a postsynaptic complex with both signal ends (Agrawal and Schatz, 1997) and hairpin coding ends (Hiom and Gellert, 1998) suggests that these processing events are likely to proceed within a controlled synaptic complex, it cannot be excluded that the 5′ flap endonuclease FEN-1 (Harrington and Lieber, 1994) and the complex of Mre11/Rad50/Nbs1 (Paull and Gellert, 1999) contribute to the processing of coding ends.

A Common DNA Structural Motif Links the Mechanisms of Sequence-Specific RSS Nicking and Flap Removal

The corresponding effects of RAG2 and C-terminal RAG1 mutants on RSS and flap nicking support our previous conclusion that RAG1/RAG2 contain a single active site responsible for both sequence-dependent and independent nicking events (Besmer et al., 1998). How can a single active site effectively process the seemingly disparate RSS substrates and coding end structures required for generating both combinatorial and junctional diversity? Our data demonstrate that activation of the hydrolytic mechanism of RAG1/RAG2 requires a common structural intermediate, a ds/ss junction. Upon binding of RAG1/RAG2, RSSs are likely distorted at the heptamer/coding flank border to form such an intermediate. The strict requirement for a CACA at this border likely results from the propensity of such sequences to facilitate melting and form such ds/ss intermediates. Accordingly, introduction of mispaired bases within the heptamer activates both binding and nicking (Figure 6). This distortion may mimic a transitional DNA structure attained during RSS recognition that directs site-specific nicking by RAG1/RAG2. We suggest, as depicted in Figure 7B, that all known hydrolysis reactions mediated by RAG1/RAG2 are likely to occur on ds/ss DNA junctions that position and trigger the nicking mechanism of the RAG1/RAG2 active site. Alternatively, the active site of RAG1/RAG2 may alter

its structure to accommodate partially different DNA substrates during the multiple hydrolysis reactions that they perform.

Mechanistic Conservation of 3′ Flap Activity in Transpositional Recombination: Implications for Excision Site Processing

The observation that Tn10 transposition involves transposase-mediated hairpin formation and resolution (Kennedy et al., 1998) suggests a connection between the mechanisms of V(D)J and transpositional recombination. In this report, we extend these mechanistic parallels by demonstrating that Tn10 can also function as a 3′ flap endonuclease. While a role for branched 3′ intermediates has yet to be defined during Tn10 transposition, it is conceivable that such intermediates may exist during the Tn10 insertion reaction. More importantly, the conservation of flap activity between RAG1/RAG2 and Tn10 strongly implies that other transposases may contain 3′ flap endonuclease activities that directly process transpositional intermediates. RAG1/RAG2 and Tn10 conceivably represent the inaugural members of a large family of sequence-specific recombinases/transposases possessing structure-specific 3′ flap endonuclease activities.

A potential role for 3′ flap removal is evident during the transposition reactions of the hAT family of transposons. The members of this family of mobile genetic elements include maize transposons of the Activator-Dissociation (Ac-Ds) family and the suppressor mutator (Spm) family, as well as *Antirrhinum majus* plant transposons Tam1–Tam4, *Linum usitatissimum* flax plant transposon dLute, and the *Ascobolus immersus* fungal transposon Ascot-1, which all leave DNA footprints at the sites of excision (reviewed by Coen et al., 1989 and Federoff, 1989; Colot et al., 1998; Luck et al., 1998). Given that the original sequence of the insertion site is not reconstituted following imprecise transposon excision, transposition permanently alters the host's genome and potentiates genetic evolution of the organism. Interestingly, the genetic alterations observed at these excision sites are fundamentally similar to the junctional diversity noted at the coding borders following deletion/excision of intervening DNA during V(D)J recombination. The most extensively characterized excision sites of the hAT transposon family are those of Ascot-1 that demonstrate palindromic nucleotides, short deletions, and end joining directed by regions of short homology within 3′ overhangs (Colot et al., 1998). Compelling evidence favors a model whereby generation of excision junctions requires hairpin formation followed by asymmetric hairpin resolution to form 3′ overhangs (Coen et al., 1989; Colot et al., 1998). The apparent mechanistic conservation of 3′ flap endonuclease activity between RAG1/RAG2 and Tn10 raises the intriguing possibility that processing and resolution of such junctional-branched intermediates may be mediated by a 3′ flap activity intrinsic to transposases. This suggests a basic parallel in the molecular mechanisms for the generation of diversity in transposon-mediated genomic evolution and the diversification of antigen receptors in the immune system.

Experimental Procedures

DNA Nicking Substrates

Overhang nicking substrates were generated by annealing depicted oligonucleotides (Figure 1A). The upper strand was 3′ end labeled with ^{32}P deoxyadenosine triphosphate (cordecypin, NEN), with TdT increasing the overhang length by 1 nucleotide, and annealed to 5-fold excess unlabeled complementary oligonucleotides. Nicking activity of wild-type and mutant RAG1 and RAG2 proteins was assayed on substrate 12 RSS (Besmer et al., 1998).

3′ flap structures (FLAP1 and FLAP2), the double-stranded counterpart (DS), and the NHEJ structure were assembled with oligonucleotides (1: 5′-GGATTTAGGAGCCTCTTCGGCGCTAA-3′; 2: 5′-TATTACTCCCC-3′; 3: 5′-GGGGAGTAATACGCCGAAGAGGTTGAC3′; 4: 5′-CTCCTAAATCC-3′; 5: 5′-GGATTTAGGAGCCTCTTCGGCGTATTACTCCCC-3′; 6: 5′-GGGGAGTAATACGCCGAAGAGGCTCCTAAATCC-3′) in the following combinations: FLAP1 (1/2/6), FLAP2 (3/4/5), DS (5/6) and NHEJ (1/2/3/4), labeled at the indicated position.

WT 12 RSS (Figure 6A) was 5′ ^{32}P end labeled on the upper strand and annealed to fully complementary unlabeled lower strand.

A 2–base pair heptamer mutation (substrate MUT 12 RSS) was made by annealing oligonucleotides HEPTupMUT: 5′-ACGCGTCGACGTCTTAGTCAGTGATACAGCCCTGAACAAAAACCGGATCCGCG-3′ and HEPTloMUT: 5′-CGCGGATCCGGTTTTTGTTCAGGGCTGTATCACTGACTAAGAC GTCGACGCGT-3′.

Mismatches in the RSS were made by annealing ^{32}P 5′ end labeled oligonucleotide HeptupMUT to a 5-fold excess of lower strand oligonucleotides: MIS 1: 5′-CGCGGATCCGGTTTTTGTTCAGGGCTGTATCACTGATTAAGACGTCGACGCGT-3′; MIS 1,2: 5′-CGCGGATCCGGTTTTTGTTCAGGGCTGTATCACTGGTTAAGACGTCGACGCGT-3′; MIS 1/3: 5′-CGCGGATCCGGTTTTTGTTCAGGGCTGTATCACTCGTTAAGACGTCGACGCGT-3′; MIS −3/−1: 5′-CGCGGATCCGGTTTTTGTTCAGGGCTGTATCACTGACCTCGACGTCGACGCGT-3′; MIS 4/6: 5′-CGCGGATCCGGTTTTTGTTCAGGGCTGTATCCGAGACTAAGAC GTCGACGCGT-3′; MIS 7/9: 5′-CGCGGATCCGGTTTTTGTTCAGGGCTGTCGTACTGACTAAGACGTCGACGCGT-3′.

Protein Expression and Purification

Glutathione-S-transferase fusions of core murine and human RAG1 (aa 380–1040) and core murine RAG2 (aa 1–383) and full-length human RAG2 were prepared as published (Villa et al., 1998). The mutations reported in this paper were identified as previously described (Villa et al., 1998). Protein concentration was quantified by Coomassie staining following SDS-PAGE. Nuclease assays contained equal amounts of wild-type or mutant proteins. Serial N terminal deletions of RAG1 were made by PCR and verified by sequencing. Wild-type and mutant Tn10 proteins were purified as published (Kennedy et al., 1998). All the RAG and Tn10 mutant proteins were efficiently expressed and purified.

DNA Nuclease Reactions

Nicking of 12 RSS substrates was as previously described (Santagata et al., 1998). Nuclease assays on overhang, flap, and NHEJ structures were in 50 mM Tris (pH 8.0), 10 mM DTT, and either 2.5 mM Mg^{2+} or Mn^{2+} using 1 μl of coexpressed RAG1/RAG2 proteins (100 ng/μl) in a 10 ml final volume with 0.05 pmol DNA. Reactions containing Mn^{2+} or Mg^{2+} were incubated at 37°C for 10 or 60 min, respectively. For alcoholysis studies, 12% or 20% (v/v) 1,2-ethanediol or glycerol was added in a 10 ml final volume with 2.5 mM Mn^{2+} for 60 min at 37°C. Alcoholysis reactions were resolved on 22.5% polyacrylamide urea gels. Tn10 nuclease assays were as previously described (Kennedy et al., 1998).

Electrophoretic Mobility Shift Assays

DNA binding was assayed with 0.05 pmol of ^{32}P 5′ end labeled substrate and 50 ng individually expressed RAG1 and RAG2 proteins (Santagata et al., 1998). Binding reactions with wild-type and mutant 12 RSS probes were in 1 mM $MgCl_2$ with competitor DNA and binding to overhangs and flaps in 1 mM $CaCl_2$ without competitor DNA.

Acknowledgments

This paper is dedicated to the memory of Eugenia Spanopoulou and Andrew Hodtsev. S. S. is grateful to Stuart Aaronson for guidance and support. We thank Dario Strina for his dedicated work in identifying OS and SCID alleles, members of the Cortes lab for valuable discussions, Larry Shapiro, Juan Carcamo, and Jorge Mansilla-Soto for critical reading of the manuscript and Jose Trincao for his kind help. S. S. is supported by DOA/DOD Breast Cancer Predoctoral Training grant DAMD 1794-J-4111 and NIH Grant AI40191 and Cancer Research Institute Investigator Award to Z-Q. P. P. C. is supported by grants from the Arthritis Foundation and the NIH (GM45996) and D. B. H. from grants from the Medical Research Council of Canada. M. N. is supported by the NIH and is an associate investigator of the HHMI. This work was partially supported by a Telethon grant (E 917) to A. V. and is part of a Genome Project funded by Cariplo (38), Italy.

Received July 12, 1999; revised August 30, 1999.

References

Agrawal, A., and Schatz, D.G. (1997). RAG1 and RAG2 form a stable postcleavage synaptic complex with DNA containing signal ends in V(D)J recombination. Cell *89*, 43–53.

Agrawal, A., Eastman, Q.M., and Schatz, D.G. (1998). Transposition mediated by RAG1 and RAG2 and its implications for the evolution of the immune system. Nature *394*, 744–751.

Aidinis, V., Bonaldi, T., Beltrame, M., Santagata S., Bianchi, M.E., and Spanopoulou, E. (1999). The homeodomain of RAG1 recruits HMG1,2 to facilitate RSS binding and bending. Mol. Cell Biol. *19*, 6532–6542.

Akamatsu, Y., and Oettinger, M.A. (1998). Distinct roles of RAG1 and RAG2 in binding the V(D)J recombination signal sequences. Mol. Cell Biol. *18*, 4670–4678.

Besmer, E., Mansilla-Soto, J., Cassard, S., Sawchuk, D.J., Brown, G., Sadofsky, M., Lewis, S.M., Nussenzweig, M.C., and Cortes, P. (1998). Hairpin coding end opening is mediated by RAG1 and RAG2 proteins. Mol. Cell *2*, 817–828.

Bolland, S., and Kleckner, N. (1996). The three chemical steps of Tn10/IS10 transposition involve repeated utilization of a single active site. Cell *84*, 223–233.

Coen, E., Robbins, T., Almeida, J., Hudson, A., and Carpenter, R. (1989). Consequences and mechanisms of transposition in *Antirrhinum majus*. In Mobile DNA, D.E. Berg and M. M. Howe, eds. (Washington, D.C.: American Society for Microbiology), pp. 413–436.

Colot, V., Haedens, V., and Rossignol, J.L. (1998). Extensive, nonrandom diversity of excision footprints generated by Ds-like transposon Ascot-1 suggests new parallels with V(D)J recombination. Mol. Cell Biol. *18*, 4337–4346.

Cuomo, C.A., Mundy, C.L., and Oettinger, M.A. (1996). DNA sequence and structure requirements for cleavage of V(D)J recombination signal sequences. Mol. Cell Biol. *16*, 5683–5690.

Difilippantonio, M.J., McMahan, C.J., Eastman, Q.M., Spanopoulou, E., and Schatz, D.G. (1996). RAG1 mediates signal sequence recognition and recruitment of RAG2 in V(D)J recombination. Cell *87*, 253–262.

Eastman, Q.M., Leu, T.M.L., and Schatz, D.G. (1996). Initiation of V(D)J recombination in vitro obeying 12/23 rule. Nature *380*, 85–88.

Eastman, Q.M., Villey, I.J., and Schatz, D.G. (1999). Detection of RAG protein-V(D)J recombination signal interactions near the site of DNA cleavage by UV cross-linking. Mol. Cell Biol. *19*, 3788–3797.

Ezekiel, U.R., Sun, T., Bozek, G., and Storb, U. (1997). The composition of coding joints formed in V(D)J recombination is strongly affected by the nucleotide sequence of the coding ends and their relationship to the recombination signal sequences. Mol. Cell Biol. *17*, 4191–4197.

Federoff, N.V. (1989). Maize transposable elements. In Mobile DNA, D.E. Berg and M.M. Howe, eds. (Washington, D.C.: American Society for Microbiology), pp. 375–411.

Gauss, G.H., and Lieber, M.R. (1996). Mechanistic constraints on diversity in human V(D)J recombination. Mol. Cell Biol. *16*, 258–269.

Gerstein, R.M., and Lieber, M.R. (1993). Extent to which homology can constrain coding exon junctional diversity in V(D)J recombination. Nature *363*, 625–627.

Harrington, J.J., and Lieber, M.R. (1994). The characterization of a mammalian DNA structure-specific endonuclease. EMBO J. *13*, 1235–1246.

Hiom, K., and Gellert, M. (1997). A stable RAG1-RAG2-DNA complex that is active in V(D)J cleavage. Cell *88*, 65–72.

Hiom, K., and Gellert, M. (1998). Assembly of a 12/23 paired signal complex: a critical control point in V(D)J recombination. Mol. Cell *1*, 1011–1019.

Hiom, K., Melek, M., and Gellert, M. (1998). DNA transposition by the RAG1 and RAG2 proteins: a possible source of oncogenic translocations. Cell *94*, 463–470.

Kennedy, A.K., Guhathakurta, A., Kleckner, N., and Haniford, D.B. (1998). Tn10 transposition via a DNA hairpin intermediate. Cell *95*, 125–134.

Kim, D.R., and Oettinger, M.A. (1998). Functional analysis of coordinated cleavage in V(D)J recombination. Mol. Cell Biol. *18*, 4679–4688.

Landau, N.R., Schatz, D.G., Rosa, M., and Baltimore, D. (1987). Increased frequency of N-region insertion in a murine pre-B cell line infected with a terminal deoxynucleotidyl transferase retroviral expression vector. Mol. Cell Biol. *7*, 3237–3243.

Leu, T.M., Eastman, Q.M., and Schatz, D.G. (1997). Coding joint formation in a cell-free V(D)J recombination system. Immunity *7*, 303–314.

Lewis, S.M. (1994). The mechanism of V(D)J joining: lessons from molecular, immunological and comparative analysis. Adv. Immunol. *56*, 27–150.

Lieber, M.R. (1999). The biochemistry and biological significance of nonhomologous DNA end joining: an essential repair process in multicellular eukaryotes. Genes Cells *4*, 77–85.

Livak, F., and Schatz, D.G. (1997). Identification of V(D)J recombination coding end intermediates in normal thymocytes. J. Mol. Biol. *267*, 1–9.

Luck, J.E., Lawrence, G.J., Finnegan, E.J., Jones, D.A., and Ellis, J.G. (1998). A flax transposon identified in two spontaneous mutant alleles of the L6 rust resistance gene. Plant J. *16*, 365–369.

McBlane, J.F., van Gent, D.C., Ramsden, D.A., Romeo, C., Cuomo, C.A., Gellert, M., and Oettinger, M.A. (1995). Cleavage at a V(D)J recombination signal requires only RAG1 and RAG2 proteins and occurs in two steps. Cell *83*, 387–395.

Milne, G.T., Jin, S., Shannon, K.B., and Weaver, D.T. (1996). Mutations in two Ku homologs define a DNA end-joining repair pathway in Saccharomyces cerevisiae. Mol. Cell Biol. *16*, 4189–4198.

Mombaerts, P., Iacomini, J., Johnson, R.S., Herrup, K., Tonegawa, S., and Papaioannou, V.E. (1992). RAG-1-deficient mice have no mature B and T lymphocytes. Cell *68*, 869–877.

Nadel, B., and Feeney, A.J. (1997). Nucleotide deletion and P addition in V(D)J recombination: a determinant role of the coding-end sequence. Mol. Cell Biol. *17*, 3768–3778.

Nagawa, F., Ishiguro, K., Tsuboi, A., Yoshida, T., Ishikawa, A., Takemori, T., Otsuka, A.J., and Sakano, H. (1998). Footprint analysis of the RAG protein recombination signal sequence complex for V(D)J type recombination. Mol. Cell Biol. *18*, 655–663.

Oettinger, M.A., Schatz, D.G., Gorka, C., and Baltimore, D. (1990). RAG-1 and RAG-2, adjacent genes that synergistically activate V(D)J recombination. Science *248*, 1517–1523.

Patel, D.J., Shapiro, L., and Hare, D. (1987). NMR distance geometry studies of helical errors and sequence dependent conformations of DNA in solution. In Unusual DNA Structures, R.D. Wells and S.C. Harvey, eds. (New York: Springer-Verlag), pp. 115-161.

Paull, T.T., and Gellert, M. (1999). Nbs1 potentiates ATP-driven DNA unwinding and endonuclease cleavage by the Mre11/Rad50 complex. Genes Dev. *13*, 1276–1288.

Ramsden, D.A., and Gellert, M. (1995). Formation and resolution of double-strand break intermediates in V(D)J rearrangement. Genes Dev. *9*, 2409–2420.

Ramsden, D.A., McBlane, J.F., van Gent, D.C., and Gellert, M. (1996). Distinct DNA sequence and structure requirements for the two steps of V(D)J recombination signal cleavage. EMBO J. *15*, 3197–3206.

Ramsden, D.A., Paull, T.T., and Gellert, M. (1997). Cell-free V(D)J recombination. Nature *388*, 488–491.

Roth, D.B., Zhu, C., and Gellert, M. (1993). Characterization of broken DNA molecules associated with V(D)J recombination. Proc. Natl. Acad. Sci. USA *90*, 10788–10792.

Santagata, S., Aidinis, V., and Spanopoulou, E. (1998). The effect of Me2+ cofactors at the initial stages of V(D)J recombination. J. Biol. Chem. *273*, 16325–16331.

Sawchuk, D.J., Weis-Garcia, F., Malik, S., Besmer, E., Bustin, M., Nussenzweig, M.C., and Cortes, P. (1997). V(D)J recombination: modulation of RAG1 and RAG2 cleavage activity on 12/23 substrates by whole cell extract and DNA-bending proteins. J. Exp. Med. *185*, 2025–2032.

Schatz, D.G., Oettinger, M.A., and Baltimore, D. (1989). The V(D)J recombination activating gene, RAG-1. Cell *59*, 1035–1048.

Schlissel, M.S. (1998). Structure of nonhairpin coding-end DNA breaks in cells undergoing V(D)J recombination. Mol. Cell Biol. *18*, 2029–2037.

Schlissel, M., Constantinescu, A., Morrow, T., Baxter, M., and Peng, A. (1993). Double-strand signal sequence breaks in V(D)J recombination are blunt, 5′-phosphorylated, RAG-dependent, and cell cycle regulated. Genes Dev. *7*, 2520–2532.

Schwarz, K., Gauss, G.H., Ludwig, L., Pannicke, U., Li, Z., Lindner, D., Friedrich, W., Seger, R.A., Hansen-Hagge, T.E., Desiderio, S., Lieber, M.R., and Bartram, C.R. (1996). RAG mutations in human B cell-negative SCID. Science *274*, 97–99.

Shinkai, Y., Rathbun, G., Lam, K.P., Oltz, E.M., Stewart, V., Mendelsohn, M., Charron, J., Datta, M., Young, F., Stall, A.M., et al. (1992). RAG-2-deficient mice lack mature lymphocytes owing to inability to initiate V(D)J rearrangement. Cell *68*, 855–867.

Shockett, P.E., and Schatz, D.G. (1999). DNA hairpin opening mediated by the RAG1 and RAG2 proteins. Mol. Cell Biol. *19*, 4159–4166.

Spanopoulou, E., Zaitseva, F., Wang, F.H., Santagata, S., Baltimore, D., and Panayotou, G. (1996). The homeodomain region of Rag-1 reveals the parallel mechanisms of bacterial and V(D)J recombination. Cell *87*, 263–276.

Steen, S.B., Gomelsky, L., and Roth, D.B. (1996). The 12/23 rule is enforced at the cleavage step of V(D)J recombination in vivo. Genes Cells *1*, 543–553.

Swanson, P.C., and Desiderio, S. (1998). V(D)J recombination signal recognition: distinct, overlapping DNA-protein contacts in complexes containing RAG1 with and without RAG2. Immunity *9*, 115–125.

Swanson, P.C., and Desiderio, S. (1999). RAG-2 promotes heptamer occupancy by RAG-1 in the assembly of a V(D)J initiation complex. Mol. Cell Biol. *19*, 3674–3683.

Tonegawa, S. (1983). Somatic generation of antibody diversity. Nature *302*, 575–581.

van Gent, D.C., Mizuuchi, K., and Gellert, M. (1996). Similarities between initiation of V(D)J recombination and retroviral integration. Science *271*, 1592–1594.

Villa, A., Santagata, S., Bozzi, F., Giliani, S., Frattini, A., Imberti, L., Gatta, L.B., Ochs, H.D., Schwarz, K., Notarangelo, L.D., Vezzoni, P., and Spanopoulou, E. (1998). Partial V(D)J recombination activity leads to Omenn syndrome. Cell *93*, 885–896.

West, R.B., and Lieber, M.R. (1998). The RAG-HMG1 complex enforces the 12/23 rule of V(D)J recombination specifically at the double-hairpin formation step. Mol. Cell Biol. *18*, 6408–6415.